Targeting intracellular, multi-drug resistant *Staphylococcus aureus* with guanidinium polymers by elucidating the structure-activity relationship

Agnès Kuroki,[a] Arnaud Kengmo Tchoupa,[b] Matthias Hartlieb,[a †] Raoul Peltier,[a] Katherine Locock,[c,d] Meera Unnikrishnan,[b] Sébastien Perrier [a,e*]

[a] Department of Chemistry, University of Warwick, Coventry, UK

[b] Warwick Medical School, University of Warwick, Coventry, UK

[c] CSIRO Manufacturing, Clayton, Victoria, Australia

[d] Department of Chemical and Biomolecular Engineering, University of Melbourne, Melbourne, VIC 3010, Australia

[e] Faculty of Pharmacy and Pharmaceutical Sciences, Monash University, 381 Royal Parade, Parkville, Victoria, Australia

† Current Address: Institute of Biomaterial Science, Helmholtz-Zentrum Geesthacht, Kantstr. 55, 14513 Teltow, Germany

Keywords Antimicrobial, intracellular bacteria, block copolymers, RAFT polymerization;

Abstract

Intracellular persistence of bacteria represents a clinical challenge as bacteria can thrive in an environment protected from antibiotics and immune responses. Novel targeting strategies are critical in tackling antibiotic resistant infections. Synthetic antimicrobial peptides (SAMPs) are interesting candidates as they exhibit a very high antimicrobial activity. We first compared the activity of a library of ammonium and guanidinium polymers with different sequences (statistical, tetrablock and diblock) synthesized by RAFT polymerization against methicillin-resistant *S. aureus* (MRSA) and methicillin-sensitive strains (MSSA). As the guanidinium SAMPs were the most potent, they were used to treat intracellular *S. aureus* in keratinocytes. The diblock structure was the most active, reducing the amount of intracellular MSSA and MRSA by two-fold. We present here a potential treatment for intracellular, multi-drug resistant bacteria, using a simple and scalable strategy.

1. Introduction

Staphylococcus aureus is one of the major causes of both community and hospital-acquired infections, methicillin-resistant *S. aureus* (MRSA) being associated with a mortality rate fivefold higher than that of methicillin-sensitive strains (MSSA) amongst patients in Europe.[1-2] This issue is exacerbated with the ability of *S. aureus* to persist intracellularly.[3-4] The presence of *S. aureus* inside epithelial and phagocytic cells has been associated with skin infections, tonsillitis and rhinosinusitis.[5-8] Unfortunately, the most commonly used antibiotics (such as vancomycin, oxacillin, and gentamycin) are not effective against intracellular bacteria as they are not efficiently internalized by the hosts cells, which allows *S. aureus* to survive.[9-10] [9-10] In order to overcome this barrier, antibiotic loaded liposomes and nanoparticles have been explored.[11] These systems were internalized by infected mammalian cells

and efficiently killed intracellular bacteria.[12-13] To circumvent the challenges associated with the stability and the drug loading efficiency of nanoparticles and liposomes, recent work has been focusing on the use of small molecule vectors capable of promoting intracellular delivery of antibiotics.[14] Amongst those systems, cell penetrating peptides (CPPs) conjugated to antibiotics significantly reduced bacterial growth in intracellular environments.[15-16] However, the rapid development of resistance against antibiotics calls for more sustainable treatment.[12, 17-19]

Antimicrobial peptides (AMPs) have been extensively investigated as their hydrophobic and cationic residues appear to efficiently disrupt bacterial membranes. Therefore, various studies have looked into their synthetic counterparts to improve their versatility and scalability.[20-24] More importantly, synthetic antimicrobial peptides (SAMPs) seem to reduce the chance of bacteria developing resistance as they target bacterial membrane, as opposed to highly specific functions.[25-26] Previous reports demonstrated that ammonium and guanidinium-rich SAMPs were potent against a wide spectrum of bacteria.[27] Among those, arginine mimicking materials seemed particularly active against MRSA.

In parallel, a range of guanidinium containing polymers were also synthesized to mimic CPPs.[28-30] Although the mechanism of cell uptake has not been entirely elucidated, the guanidine moieties are thought to interact with membrane lipids *via* electrostatic interactions and H-bonds, followed by both endocytosis and direct diffusion through the membrane.[31] The stereochemistry of the backbone was demonstrated not to impair the internalisation of the guanidinium polymers, but other parameters such as the number of guanidinium units or the overall hydrophobicity of the polymer were reported to alter cellular uptake.[29, 32] By exploiting their antimicrobial activity of guanidinium rich polymers in combination with their ability to enter eukaryotic cells, this class of materials could be a promising alternative to antibiotics currently used against intracellular bacteria.[33-34] In this case, the usual drawbacks associated with the use of a cargo such as drug attachment/ encapsulation or release would be bypassed, as the polymer is simultaneously holding a role of vector and drug. A guanidinium SAMP, polyhexamethylene biguanidine (PHMB), which is utilized as a disinfectant, has been reported to be efficient against intracellular *S. aureus* in keratinocytes.[35-36] However, reports of its potential carcinogenic effects on humans, and increasing regulation over its use highlight the need for an alternative to PHMB.[37] In the light of recent studies, improvement of the biological properties of this material can be obtained by modifying the distribution of cationic and hydrophobic functionalities along the backbone.[38-39] Indeed, the segregation of the cationic and hydrophobic moieties appear to enhance the bactericidal effect, yet PHMB has an alternating sequence inherent to the nature of its synthesis. Varying the sequence of guanidinium containing polymers could potentially improve their intracellular activity. Therefore, the use of controlled polymerization techniques could provide viable alternatives to PHMB.

Previous reports described the synthesis of guanidinium containing polymers by post-polymerization functionalisation.[34, 40] Guanidinium monomers could also be directly polymerized with or without Boc protecting groups using ROMP or RAFT.[28, 32, 41-42] In addition to be suitable for various types of monomers, the latter technique has been utilized to prepare polymers with precisely defined compositions and narrow molar mass distributions.[43-45]

Here, we synthesized ammonium and guanidinium containing SAMPs and studied their activity against MSSA and MRSA as well as their toxicity towards mammalian cells. Additionally, SAMPs with different monomer distributions (statistical, tetrablock and diblock) were synthesized *via* RAFT polymerization in order to establish a structure-activity relationship towards *S. aureus*. Our data demonstrate that these novel SAMPs are active against intracellular *S. aureus* within keratinocytes, indicating excellent potential in staphylococcal skin infection therapy.

2. Materials and Methods

2.1. Materials

Acryloyl chloride, boron trifluoride diethyl etherate ($BF_3.OEt_2$), chloroform ($CHCl_3$), dichloromethane (DCM), dicyano-1,4-benzoquinone (DDQ), 1,4-dioxane, ethylacetate (EtOAc), ethylenediamine, 1-Ethyl-3-(3-dimethylaminopropyl)carbodiimide (EDC), *N*-hydroxysuccinimide (NHS), triethylamine (NEt_3) and trifluoro acetic acid (TFA) were purchased from Sigma-Aldrich and used without further purification. 2,2'-azobis[2-(2-imidazolin-2-yl)propane]dihydrochloride (VA-044, Wako), 4-carboxybenzaldehyde (Alfa-Aesar), 2,4-dimethylethylpyrrole (Acros Organic) and propidium iodide (PI, Thermo-Fisher) were also used without further purification. Mili-Q water was directly used as a solvent for polymerizations. *N*-isopropylacrylamide (NIPAM, Sigma-Aldrich, 97 %) was used after purification by recrystallization in *n*-hexane. Nutrient Agar, Dulbecco's Modified Eagle's Medium (DMEM), Müller-Hinton Broth (MHB), Roswell Park Memorial Institute medium (RPMI-1640) , Phosphate Buffered Saline (PBS) tablets, Trypsic Soy Broth (TSB), Concanavalin A (Con A) and Triton X were purchased from Sigma-Aldrich. 96-well plates were sourced from Thermo-Fischer. Milli-Q filtered water was used to prepare solutions, according to their recommended concentration and the solutions were autoclaved prior to their usage in order to ensure sterility. Defibrinated sheep blood was obtained from Fisher Scientific. *S. aureus* strains USA 300 LAC JE2 and NCTC 8325 RN1 were from BEI Resources, USA.

2.2. Nuclear Magnetic Resonance (NMR) Spectroscopy.

^{1}H NMR spectra were recorded on a Bruker Advance 300 spectrometer (300 MHz) at 27 °C in DMSO, $CDCl_3$ or D_2O. For ^{1}H NMR, the delay time (dl) was 2 s. Chemical shift values (δ) are reported in ppm. The residual proton signal of the solvent was used as internal standard.

2.3. Size exclusion chromatography (SEC).

Molar mass distributions were measured using an Agilent 390-LC MDS instrument equipped with differential refractive index (DRI), viscometry (VS), dual angle light scatter (LS) and dual wavelength UV detectors. The system was equipped with 2 x PLgel Mixed D columns (300 x 7.5 mm) and a PLgel 5 µm guard column. The eluent was DMF with 5 mmol NH_4BF_4 additive. Samples were run at 1 mL min^{-1} at 50°C. Poly(methyl methacrylate) standards (Agilent EasyVials) were used for calibration. Analyte samples were filtered through a nylon membrane with 0.22 µm pore size before injection. Respectively, experimental molar mass ($M_{n,SEC}$) and dispersity ($Đ$) values of synthesized polymers were determined by conventional calibration using Agilent GPC/SEC software.

2.4. *Mass spectrometry (MS).*

MS analysis was carried out with Agilent1100 HPLC coupled with Agilent 6130B single quadruple mass spectrometer equipped with electrospray ionisation source. Mobile phases is 80% methanol with 20% water at flow rate at 0.2 mL.min^{-1}. Mass spectrometer was operated in electrospray positive ion mode with a scan range 50-500 m/z. Source conditions are: capillary at 4000V; nebulizer gas (N_2) at 15 psi; dry gas (N_2) at 7 L.min^{-1}; Temperature at 300 °C. Calibration was done with ESI tuning mix from Agilent.

2.5. Fluorescence spectrometer.

The fluorescent intensity was monitored using Agilent Technologies Cary Eclipse Fluorescence Spectrophotometer. The solutions of vesicles were introduced in a polystyrene cuvette for the measurements.

2.6. High performance liquid chromatography (HPLC).

HPLC was performed using an Agilent 1260 infinity series stack equipped with an Agilent 1260 binary pump and degasser. The flow rate was set to 1.0 mL min^{-1} and samples were injected using Agilent 1260 autosampler with a 100 µL injection volume. The temperature of the column was set at 37 °C. The HPLC was fitted with an Agilent C18 column (100 x 4.6 mm) with 5 micron packing (100Å). Detection was achieved using an Agilent 1260 variable wavelength detector. UV detection was monitored at λ = 309 nm. Methods were edited and run using Agilent OpenLAB online software and data was analysed using Agilent OpenLAB offline software. Mobile phase solvents used were HPLC

grade (ACN was 'far UV') and consisted of mobile phase A: 100 % ACN, 0.04 % TFA; mobile phase B: 100 % water, 0.04 % TFA with a gradient of 1 to 80 % ACN over 30 minutes.

2.7. Dynamic Light Scattering (DLS) measurements.

DLS measurements were taken using a Malvern instruments Zetasizer Nano at 37 °C with a 4 mW He-Ne 633 nm laser at a scattering angle of 173° (back scattering). For DLS aggregation studies, 1.024 mg of polymer sample was dissolved in 1 mL of PBS buffer at pH 7.4 and a total of 0.5 mL of the solution was introduced in a 1.5 mL polystyrene cuvette after filtering with a 0.2 μm filter**.**

2.8. Synthesis of N-t-butoxycarbonyl-N'-acryloyl-1,2-diaminoethane BocAEAM.

The synthesis and polymerization conditions of BocAEAM has been described in a previous publication.[39]

2.9. Synthesis of 2-[1,3-Bis(tert-butoxycarbonyl)guanidine]ethyl acrylamide (diBocGEAM0.

The description of the synthesis of diBocGEAM can be found in the supplementary data.

2.10. Typical synthesis of the statistical copolymer.

Monomer(s), initiator, CTA and solvents were introduced in a test tube equipped with a mechanical stirrer and a rubber septum (Table SI-2 for the quantity of reagents needed for the statistical copolymers). The solution was degassed with nitrogen for *ca*. 15 min and the polymerization was then performed in a thermostated oil bath. After the desired polymerization time, the test tube was withdrawn from the oil bath.

2.11. Typical synthesis of block copolymers.

Typical synthesis of the initial block. Monomer, initiator, CTA and solvents were introduced in a test tube equipped with a mechanical stirrer and a rubber septum (Tables SI-3, SI-4 and SI-5 for the quantity of reagents needed for the diblock and multiblock copolymers). The solution was degassed with nitrogen for *ca.* 20 min and the polymerization was then performed in a thermostated oil bath at 46 °C. After 20 hours, the test tube was withdrawn from the oil bath and a sample was taken for ^{1}H NMR and SEC analysis.

Typical synthesis of subsequent blocks. The test tube with the reaction mixture was opened and additional monomer, initiator and solvent were introduced. After the mixture was sealed with a septum, the solution was degassed for *ca.* 20 min, then placed in an oil bath set at 70 °C for the polymerization to occur. The tube was withdrawn from the oil bath after 2 hours and a sample was taken for ^{1}H NMR and SEC analysis.

2.12. Deprotection of the polymers

The polymers were dissolved in TFA and stirred for 3 hours at 40 °C. The TFA was then removed and the polymers were precipitated in diethyl ether. In order to remove the TFA counter-ion, the polymers were dialysed against a NaCl solution, followed by dialysis against distilled water.

2.13. Synthesis of Bodipyacrylamide (BodipyAM)

The description of the synthesis of BodipyAM can be found in the supplementary data.

2.14. Chain extension of the deprotected polymers with BodipyAM

polyGEAm-*co*-NIPAm (13.9 mg, 1 μmol) was dissolved in an acetate buffer (pH 5). A solution of Bodipy acrylamide (0.5 mg, 1 μmol) in acetone was added, as well as a solution of VA-044. The reaction mixture was degassed for 15 min, then placed in an oil bath at 46 °C for 5 hours. The polymer was then precipitated in Et_2O.

2.15. *Hemolysis and hemagglutination assays*

Sheep red blood cells (RBCs) were prepared by washing defibrinated sheep blood with PBS *via* centrifugation. Polymers were dissolved in PBS. The normalisation was done using positive controls (50 μg mL^{-1} Concanavalin A for hemagglutination and 2 % Triton X-100 in PBS for hemolysis) and negative control (PBS) which were included on each plate. A suspension of 3 % in volume of RBCs was added to each well and the contents were mixed before being incubated at 37°C for 2 hours. The 96-well plates were centrifuged at 600 x *g* for 10 minutes then 100 μL of the supernatant was transferred into a new plate. The absorbance at 540 nm was measured and normalized using the positive and negative control.

2.16. Eukaryotic Cell Lines and Growth Conditions

HaCaT human keratinocytes were grown in a 50:50 mixture of Ham's F12 and Dulbecco's Modified Eagle's Medium (DMEM) supplemented with 10% of foetal calf serum, 1% of 2 mM glutamine and 1%. Both cell lines were grown as adherent monolayers at 37 °C in a 5% CO_2 humidified atmosphere and passaged at approximately 70-80% confluence.

2.17. In vitro growth inhibition assays

The anti-proliferative activity of the polymers was determined in HaCaT human keratinocytes. 96-well plates were used to seed 5000 cells per well which were left to pre-incubate with drug-free medium at 37 °C for 24 hours before adding different concentrations of the compounds to be tested (1024 μg mL^{-1} – 32 μg mL^{-1}). A drug exposure period of 24 hours was allowed. The XTT assay was used to determine cell viability. The IC_{50} values (concentrations which caused 50% of cell death), were determined as

duplicates of triplicates in two independent sets of experiments and their standard deviations were calculated.

2.18. Bacterial Strains and Growth Conditions

The utilized bacterial strains were *S. aureus* USA 300 LAC JE2 and NCTC 8325 (RN1). Bacteria were grown in TSB at 37°C at 250 rpm for 18 hours.

2.19. Antibacterial susceptibility tests

Antibacterial susceptibility was studied using two strains of *Staphylococcus aureus* (*S. aureus*): RN1 and JE2. Minimum inhibitory concentrations (MICs) were determined according to the standard Clinical Laboratory Standards Institute (CLSI) broth microdilution method (M07-A9-2012). A single colony of bacteria was picked up from a fresh (24 hour) culture plate and inoculated in 5 mL of Mueller-Hinton (MH) broth, then incubated at 37 °C overnight. On the next day, the concentration of cells was assessed by measuring the optical density at 600 nm (OD_{600}). Culture suspension was then diluted to an OD_{600} = 0.1 with MHB in order to reach a bacterial concentration of ~ 10^8 colony forming unit per mL (CFU mL^{-1}). The solution was diluted further by 100 fold to obtain a concentration of 10^6 CFU mL^{-1}. Polymers were dissolved in MHB and 100 μL of each test polymer was added to micro-wells followed by the addition of the same volume of bacterial suspension (10^6 CFU mL^{-1}). The micro-wellplates were incubated at 37 °C for 24 hours, and growth was evaluated by measuring the OD_{600} using a plate reader. Triplicates were performed for each concentration and readings were taken twice. The growth in the well was normalized using negative controls, wells without any bacteria introduced, and positive controls, wells only containing bacterial solution.

2.20. Binding assay

Interactions of fluorescent polymers with bacterial membrane was investigated using the MRSA strain of *S. aureus*. A colony was inoculated in 5 mL of TSB at 37 °C overnight. The inoculum was diluted to reach an OD=0.15, then it was incubated for 2 hours to reach OD=1. 1 mL of the suspension was centrifuged at 5000 rpm for 5 minutes. The bacteria were resuspended in a solution containing fluorescent polymer at a concentration of 128 μg.mL^{-1} in PBS. The bacteria were incubated at 37 °C for 15 minutes, 30 minutes or 2 hours whilst shaking at 500 rpm. For the experiments with PI, 15 minutes prior to the end of the incubation time, a solution of PI was added to reach a final concentration of 30 μM. At the end of the incubation time, the bacteria were centrifuged, the pellet washed with PBS, then resuspended in 100 μL of PBS, of which 5 μL was placed on an agarose gel covering a glass slide. Upon drying, 20 μL of DAPI was added and the cover slip was placed on the sample. The slides were then imaged using a Leica DMi8 fluorescence microscope equipped with a FITC filter (480nm/40) used to view BodipyAM and a TXR filter (560nm/40) to image PI.

2.21. Cell uptake assay

HaCaT cells were seeded (2 10^4 cells/well) in a black 96-well plate with clear bottom. After 24 hours, the cells were incubated with fluorescent polymers (128 and 40 μg.mL^{-1}) for 2 or 16 hours depending on the specified conditions. In order to stain the nucleus of the cells, Hoescht 33342 was added to each well 15 minutes prior to the end of the incubation time. For the experiment performed at 4 °C, the plate was placed in the fridge 30 min prior to the polymer treatment. The wells were viewed after washing and replacing with fresh media using a Cytation3 Cell Imaging Multi-Mode ReaderTM from Biotek®. Gen5^{TM} was used to isolate individual cells with the blue channel. The background was removed with a rolling ball model (20 μm) and intracellular fluorescence was determined using the RFP filter (λ_{ex} = 531 nm, λ_{em} = 593 nm) to view the Bodipy-functionalized polymers. Two separate experiments were conducted with triplicates.

2.22. Invasion assay

The intracellular infection was performed on HaCaT cells using RN1 and JE2. 24-well plates were used to seed 2 10^5 cells per well which were left to pre-incubate with antibiotic-free medium at 37 °C for 10 hours. A single colony of bacteria was inoculated in TSB at 37 °C overnight. The inoculum was diluted to reach an OD=0.15 and were incubated for 2 hours to reach OD=1. After a 1:200 dilution, 1 mL of the bacterial solution was added in each well and the cells were incubated for another 2 hours at 37 °C. The medium was then removed and the wells were washed with 1 mL of PBS. 500 μL of a solution of 50 μg.mL^{-1} of gentamicin and 20 μg.mL^{-1} of lysostaphin in DMEM was added and the plate was left at 37 °C for 30 min to kill the extracellular bacteria. The solution was removed and the wells were washed with PBS. 500 μL of polymer solution was added and the plate was incubated at 37 °C for 2 hours, using a solution of 5 μg.mL^{-1} of lysostaphin as a negative control. 1 mL of a solution of 0.5 % of saponin was added to disrupt the membrane of mammalian cells. After 10 minutes at 37 °C, serial dilution of each well in PBS was undertaken following a thorough detachment of the cells. Each serial dilution was then plated on an Agar plate and left in the incubator overnight. The number of bacteria was counted on the next day.

2.23. Statistical analysis of data

The statistical significance of the differences between cfu/mL recovered from various groups was analysed using the One-way ANOVA test. Differences were considered significant if $P \leq 0.05$.

3. Results and discussion

3.1. Synthesis and characterisation of ammonium and guanidinium polymers *via* RAFT

In order to study the effect of the type of cationic group on the polymer activity against MSSA and MRSA, we used acrylamide monomers, guanidino-ethylacrylamide (GEAM) and amino-ethylacrylamide (AEAM), mimicking arginine and lysine respectively. The acrylamide monomer family is particularly suitable for the synthesis of multiblock copolymers *via* RAFT since they possess a high rate constant of propagation (k_p) and therefore, it is possible to polymerize them to high conversion with much lower initiator concentrations than other monomer families, such as methacrylates.[46] GEAM and AEAM monomers were synthesized with Boc protecting groups (diBocGEAM and BocAEAM, respectively) in order to avoid any aminolysis of the trithiocarbonate of the RAFT agent during the polymerization process (Figures SI-1, SI-2, SI-3). BocAEAM and diBocGEAM were both obtained with high yields in two-step syntheses as described in the literature.[32, 39] They were then separately copolymerized with *N*-isopropylacrylamide (NIPAM), which in combination with AEAM at 70:30 molar ratio, has been shown to reduce the toxicity towards mammalian cells of cationic copolymers while maintaining antimicrobial properties.[39] Therefore, all polymers in this study were synthesized with 30 molar % of cationic monomer. The RAFT agent used for the synthesis was (propanoic acid)yl butyl trithiocarbonate (PABTC) as it is suitable for the polymerization of acrylamides and its synthesis is facile and scalable.[39]

For each set of monomers (BocAEAM and diBocGEAM with NIPAM), a statistical, tetrablock and diblock copolymers (Figure 1A) was synthesized to study the influence of monomer distribution on the antimicrobial activity. The final targeted degree of polymerization (DP) was 100 for all the polymers, thus the shortest cationic blocks were of DP 15 (for the tetrablocks), which is expected to be high enough to ensure that the majority of polymer chains possess the correct monomer sequence.[47] All materials will be referred below according to the type of charge (G for guanidinium and A for ammonium), the amount of charge (here 30 molar % for all the polymers), their sequence (S for statistical, T for tetrablock and D for diblock) and labelled Boc when in their protected form (Table 1).

Table 1. Synthesized Boc-protected polymers.

Co-monomer	Segmentation	Composition	Label
Amino-polymers	Statistical	$NIPAM_{70}$-*s*- $BocAEAM_{30}$	A-S30^{Boc}
	Diblock	$NIPAM_{70}$-*b*- $BocAEAM_{30}$	A-D30^{Boc}
	Tetrablock	$NIPAM_{35}$-*b*- $BocAEAM_{15}$-*b*- $NIPAM_{35}$-*b*- $BocAEAM_{15}$	A-T30^{Boc}
Guanidino-polymers	Statistical	$NIPAM_{70}$-*s*- $diBocGEAM_{30}$	G-S30^{Boc}
	Diblock	$NIPAM_{70}$-*b*- $diBocGEAM_{30}$	G-D30^{Boc}
	Tetrablock	$NIPAM_{35}$-*b*- $diBocGEAM_{15}$-*b*-$NIPAM_{35}$-*b*- $diBocGEAM_{15}$	G-T30^{Boc}

The polymerization of BocAEAM and diBocGEAM required higher initiator concentrations than for the polymerization of NIPAM. Furthermore, the first polymerization cycle generally requires a higher initiator concentration than subsequent polymerization cycles in order to fully consume the initial CTA.[48] Since the polymerization of NIPAM required lower concentrations of initiator to achieve full monomer conversion, it was selected as the first block in each block copolymer synthesis in order to preserve a higher fraction of living chains going into subsequent block extensions. The polymerization of diBocGEAM was undertaken at 46 °C since a loss of molar mass control was observed at higher temperatures. The reaction conditions were optimized to maintain a high livingness of the polymer chains, which is necessary for the synthesis of multiblock copolymers (Tables SI-1 to SI-4).[48-49] Under these conditions, full monomer conversion was reached for each chain extension, allowing for the synthesis of the block copolymers in one pot (Figures 1B and SI-4). All polymers were obtained with the targeted molar mass and a low dispersity ($Đ \leq 1.24$) according to SEC analysis (Figures 1C, SI-5 and SI-6, Table SI-5). A shift to higher molar mass after each chain extension was confirmed with the SEC traces, but in most cases the experimental molar mass $M_{n,SEC}$ did not match the theoretical one $M_{n,th}$ (Table SI-5), which can be explained by the nature of the PMMA standards used for the calibration of the instrument.

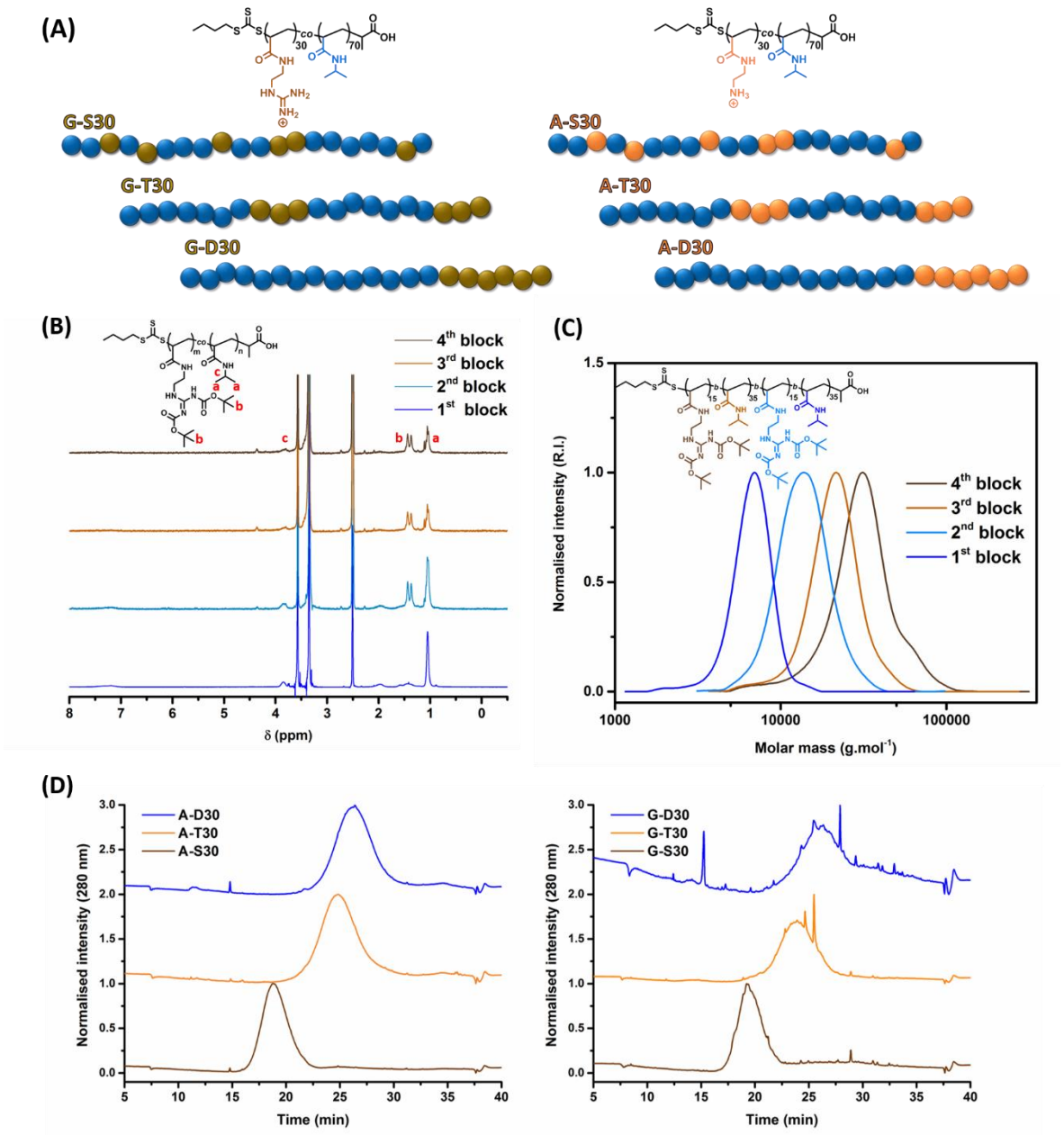

Figure 1. Synthesis of the polymer library. (A) Schematic of the ammonium and guanidinium polymer library. (B) ^{1}H NMR spectra in DMSO-d_6 of the successive chain extensions for the synthesis of G-T30^{Boc}. (C) DMF-SEC chromatograms of the successive chain extensions for the synthesis of G-T30^{Boc}. (D) RP-HPLC chromatograms of the ammonium and the guanidinium polymers with a gradient of 1 to 80 % ACN in 30 minutes with a 100 mm C18 column.

Following the polymerization process, the protected guanidinium copolymers were deprotected using TFA, with quantitative deprotection confirmed using ^{1}H NMR in D_2O (Figure SI-7). This deprotection method further justifies the choice of acrylamide monomers as they are more stable towards hydrolysis than acrylates or methacrylates.[50] The cationic polymers were then dialysed against a solution containing NaCl to replace the TFA counter-ions with Cl^- as shown by ^{19}F NMR (Figure SI-

8), and finally against distilled water to remove any traces of excess NaCl. The polymers were obtained as solids after freeze-drying.

To identify the effect of monomer distribution on the physico-chemical properties of the polymer library, which could in turn alter their biological activity, characterisation of the polymers by reverse phase HPLC (RP-HPLC) was performed (Figure 1D, Table SI-6). The elution time of the polymers can be correlated to their hydrophobicity, where earlier elution times indicate less hydrophobicity. Preceding work examining the ammonium counterparts, but also other types of polyacrylamide-based multiblock copolymers established a comparable trend between elution time of the polymers with different composition and hydrophobicity.[51] RP-HPLC of the guanidinium polymers indicated the following trend, with hydrophobicity of the polymers decreasing left to right; diblock (G-D30) > tetrablock (G-T30) > statistical (G-S30). Moreover, Hou *et al*. utilized copolymers of NIPAM and *N*-vinylcaprolactam to demonstrate that the cloud point temperature of the statistical copolymer was higher than that of the diblock.[52] This observation was attributed to the increase of the overall hydrophobicity of the polymer chain with the segregation of the monomer types along the backbone. Similarly, in the case of G-D30, G-T30 and G-S30, the size of the discreet hydrophobic segments (here the polyNIPAM block) are likely affecting the overall hydrophobicity of the polymer structures. The amphiphilic balance of cationic polymers strongly affects their membrane interactions and will not only alter their antimicrobial properties, but also their internalisation in mammalian cells.[32]

Next, the behaviour of the copolymers in solution was analysed by DLS at 37 °C and pH 7.4 at the maximum concentration tested for the biological experiments (1024 $\mu g.mL^{-1}$). Since polyNIPAM is known to possess a lower critical solution temperature (LCST) in aqueous solution close to physiological temperatures, it was pertinent to demonstrate that the copolymer do not self-assemble.[53] No self-assembly was observed for both the ammonium and guanidinium copolymers (Figure SI-9, Table SI-6). These results are in agreement with the general observation that the LCST of polymers increases when they are copolymerized with a non-temperature-responsive monomer.[54] Since no micellar formation was observed, any difference in the activity of the polymers can be directly correlated to the monomer sequence.

3.2. Synthesis of Bodipy acrylamide and fluorescent guanidinium polymers

In order to carry out binding or cell uptake assays, the guanidinium polymers were functionalized using a Bodipy dye. Bodipy-derived dyes are known to have a high quantum yield and have been extensively used to label polymers.[55] Here, we synthesized an acrylamide derivative of the Bodipy dye to incorporate into the guanidinium copolymers *via* RAFT polymerization. Firstly, Bodipy acid was synthesized after 2 steps according to the literature (Figure SI-10).[56] The obtained compound was then

modified to obtain a NHS-functionalized Bodipy (Figure SI-11). This NHS-Bodipy was then converted into an acrylamide by using the AEAM monomer, recovered from the deprotection of BocAEAM (Figure SI-12). As the AEAM monomer is not soluble in organic solvents, the Bodipy acid was functionalized with NHS in DMF before reaction with AEAM in water, to limit hydrolysis. The obtained BodipyAM was fluorescent with λ_{ex}=525 nm and λ_{em}=537 nm (Figure SI-13). The guanidinium polymers were then chain extended with one unit of BodipyAM per polymer chain using a RAFT process. The polymerizations were performed in a mixture of an acetate buffer at pH 5 to limit aminolysis and acetone to solubilize BodipyAM. The excess dye was removed by further diluting the mixture with acetone followed by a precipitation in diethyl ether. The Bodipy labelled statistical, tetrablock and diblock copolymers (G-S30^{Bodipy}, G-T30^{Bodipy} and G-D30^{Bodipy}, respectively), which contained less than 5 % of free dye, were characterized using fluorescence spectroscopy and HPLC (Figure SI-14).

3.3. Toxicity of SAMPs towards mammalian cells

Hemocompatibility of SAMPs. As cationic polymers are known to be hemotoxic, defibrinated sheep blood was used to assess the hemocompatibility of the synthesized polymers up to 1024 μg.mL^{-1} over 2 hours at 37 °C, according to an adapted protocol from the literature.[34, 57] Remarkably, none of the ammonium polymers were hemolytic in contrast to Triton X, which was used as a positive control (Figure SI-15A). Amongst the guanidinium polymers, G-D30 induced 10% hemolysis at a concentration of 1000 μg.mL^{-1}, while the statistical and tetrablock counterparts (G-S30 and G-T30) were not hemolytic within the concentration range tested (Table 2, Figure SI-15B).

Since the hemocompatibility of polymers encompasses both hemolytic and hemagglutination, the latter was studied with defibrinated sheep blood, and Concanavalin A as a positive control.[58] A-S30 and A-T30 induced hemagglutination, from concentrations of 64 and 128 μg.mL^{-1}, respectively (Table 2), whereas A-D30 did not. These results are consistent with those obtained from a previous study, where the heptablock and statistical poly(NIPAM-*co*-AEAM) also induced the formation of RBC aggregates whilst the diblock copolymer did not exhibit any toxicity.[39] These observations could be explained by the distribution of cationic functionalities along the polymer backbone facilitating the cross-linking of RBCs. Similarly, for guanidinium polymers, the aggregation of RBCs was observed with G-S30 and G-T30, from concentrations of 8 and 32 μg.mL^{-1}, respectively, while G-D30 as well as A-D30 did not induce hemagglutination (Tables SI-7 and SI-8). The polymers which induced aggregation of red blood cells (statistical and tetrablock copolymers) were not hemolytic, suggesting that each aspect of hemotoxicity are relatively independent for the investigated materials. Combined, hemolysis and hemagglutination assays revealed that the diblocks A-D30 and G-D30 were the most hemocompatible systems, whereas the statistical and tetrablocks induced hemotoxicity at low concentrations (Table 2).

Compatibility of SAMPs with human cells. As *S. aureus* was shown to persist within keratinocytes during skin infections, SAMPs need to exhibit a low toxicity towards these cells to warrant their clinical application.[2, 59] The toxicity of the two sets of polymers against human keratinocytes (HaCaT) was evaluated over a period of 24 hours using an XTT assay. The toxicity of the amine polymers towards HaCaT was surprisingly low, with an IC_{50}>1000 µg.mL^{-1} for all three compositions (Figure 2A), indicating that the monomer sequence did not influence the toxicity of these polymers at the tested concentrations. For each copolymer composition, the guanidinium polymers were shown to be more toxic than their corresponding ammonium polymers. The difference between the two tetrablock copolymers (A-T30 and G-T30) and the two diblock copolymers (A-D30 and G-D30) was particularly significant (Figure 2A). This result is in agreement with a previous reported work studying methacrylamide-based statistical copolymers containing guanidinium and ammonium moieties.[60] By increasing the ratio of guanidinium to ammonium functionalities, the toxicity of the polymers were shown to increase towards MCF-7 epithelial cells. Indeed, due to their similarity to arginine-rich CPPs, the guanidinium polymers could undergo enhanced interactions with mammalian cell membranes compared to their ammonium counterparts, which would affect their toxicity.[61] Furthermore, segregation of cationic and hydrophobic functionalities also significantly increased the toxicity of the ammonium and guanidinium SAMPs towards epithelial cells. According to the IC_{50} values (Table 2), G-D30 appeared to be the most toxic, followed by G-T30 and G-S30. The toxicity observed with each polymer composition correlates to their overall hydrophobicity (determined via RP-HPLC, Figure 1), indicating that an increase in hydrophobicity accounts for an increase in toxicity. Similarly, Neanmark and co-workers reported an increase in cytotoxicity with hydrophobicity by using poly(ethylenimine)s bearing aliphatic substituents of varying lengths.[62]

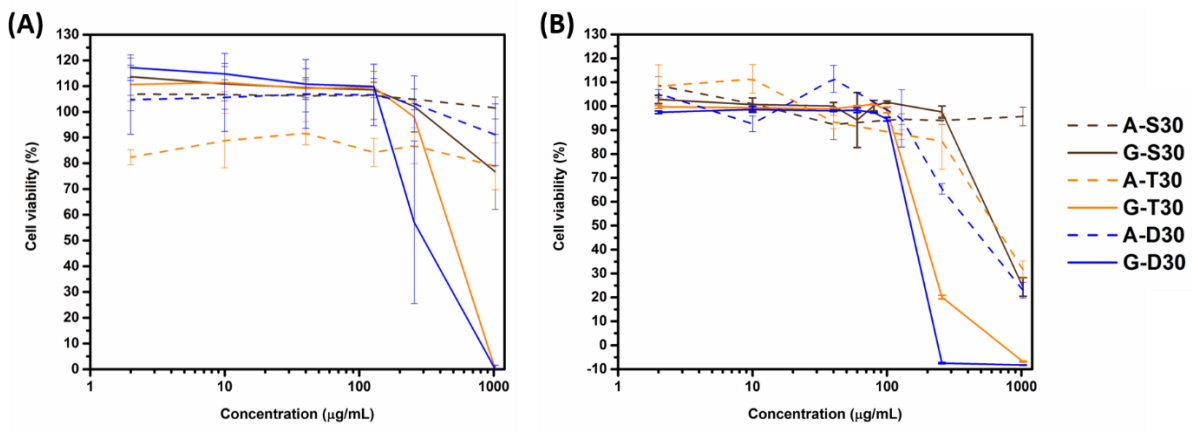

Figure 2. Cytotoxicity of ammonium and guanidinium copolymers against (A) HaCaT cells and (B) A549 cells. Cell viability after a 24-hour incubation in presence of statistical, tetrablock and diblock ammonium and guanidinium SAMPs using an XTT assay.

As pneumonia is another common ICU-acquired infection associated with *S. aureus*, the toxicity of the polymers towards lung epithelial cells (A549) was also evaluated over the course of 24 hours using an XTT assay (Figure 2B).[63] With A549 cells, A-T30 and A-D30 were found to be toxic at relatively high concentrations (IC_{50} of 700 and 400 μg.mL^{-1}), while the guanidinium counterparts were again more toxic. Similarly, the IC_{50} decreased with increasing segregation of the co-monomers (G-S30 > G-T30 > G-D30 as shown in Table 2). Taken together, the toxicity data revealed that toxicity increases with segregation, which has not been demonstrated before, to the best of our knowledge.

Table 2. Toxicity values of the SAMPs against RBCs, HaCaT and A549 cells.

	Hemocompatibility		IC_{50} [c] (μg.mL^{-1})	
	HC_{10} [a] (μg.mL^{-1})	c_H [b] (μg.mL^{-1})	HaCaT	A549
A-S30	> 1024	64	> 1024	> 1024
A-T30	> 1024	128	> 1024	700
A-D30	> 1024	> 1024	> 1024	400
G-S30	> 1024	8	> 1024	600
G-T30	> 1024	32	500	200
G-D30	1024	>1024	300	150

[a] HC_{10} is the minimum concentration at which at least 10 % of the maximum lysis was observed.

[b] c_H is the lowest concentration at which the polymers induce aggregation of RBCs.

[c] IC_{50} was determined as the concentration at which 50 % of cell growth inhibition occurred.

3.4. Antimicrobial activity of SAMPs

Two clinically relevant strains of *S. aureus* were used to evaluate their antimicrobial susceptibility towards the synthesized polymers: RN1 (NCTC 8325), a MSSA strain, which is widely used laboratory strain, and USA300 JE2, a MRSA strain, which is considered to be more virulent than RN1.[64-65]

For both the ammonium and guanidinium polymers, the monomer distribution had a significant effect on their efficacy against *S. aureus* (Table 3). MIC against RN1 decreases with the segmentation for both sets of polymers (Figures 3A and B). The ammonium and guanidinium polymers with the same sequence had similar MICs against the MSSA strain. The statistical copolymers (A-S30 and G-S30) appeared to be inactive against RN1 within the concentration range tested (MIC>1000 μg.mL^{-1}), whereas the tetrablock and diblock copolymers exhibited relatively low MIC values (from 128 and 64 μg.mL^{-1}, respectively). G-D30 an A-D30 were the most active against RN1 with a MIC of 64 μg.mL^{-1}. A similar trend was observed with the MRSA strain for both sets of polymers, as the antimicrobial

activity increased with the segregation of functionalities (Figure 3B). Strikingly, the MIC values of G-T30 and G-D30 against JE2 (128 and 64 μg.mL^{-1}, respectively) were decreased by two-fold compared to A-T30 and A-D30 (256 and 128 μg.mL^{-1}, respectively) (Figure 3B). Since the molar mass of the ammonium and guanidinium polymers are comparable (Table SI-6), the difference in the MIC values strongly suggests that the guanidinium copolymers were more potent than the ammonium counterparts, which is consistent with a previous study.[34] While the role of polymers bearing amine moieties appear to derive from their attachment to bacterial membranes followed by the formation of pores, polymers bearing guanidinium moieties could have a different antimicrobial mechanism. Indeed, the binding of guanidine units to phospholipids from bacterial membrane was shown to be more labile, hence allowing an efficient membrane crossing.[66] Recently, Good and co-workers reported that the antimicrobial activity of polyhexamethylene biguanidine is attributed to its differential access to, and subsequent condensation of, bacterial DNA over mammalian DNA, thereby inducing bacterial death.[67]

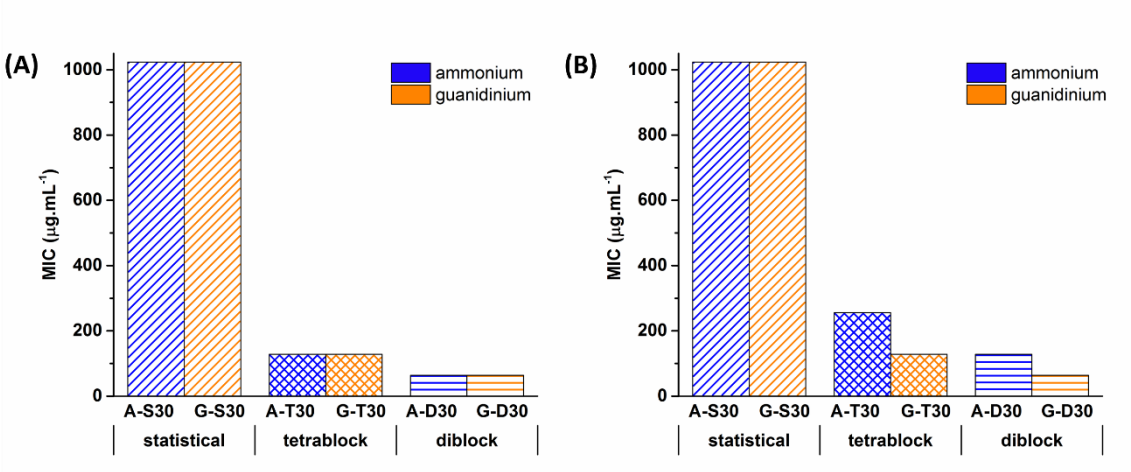

Figure 3. Antimicrobial activity of SAMPs against *S. aureus*. (A) MIC values of the ammonium and guanidinium polymers against RN1. (B) MIC values against JE2 as described in (A).

The MIC of A-T30 and A-D30 against JE2 (256 and 128 μg.mL^{-1}, respectively) was double that observed against RN1 (128 and 64 μg.mL^{-1}, respectively) as shown on Table 3. It is plausible that JE2 and RN1, by virtue of their dissimilar methicillin-susceptibility, have different membrane compositions and physical properties (thickness, surface charge), which has been shown to influence the sensitivity of bacteria towards SAMPs.[68-69] Thus, the more hydrophobic the polymer, the more toxic it is towards mammalian cells but also towards bacteria.

Table 3. Biological properties of ammonium and guanidinium SAMPs.

	MIC[a] (μg.mL^{-1})		MIC[a] (nmol.mL^{-1})		Selectivity with RBCs[b]		Therapeutic Index (TI) [c] with HaCaT	
	RN1	JE2	RN1	JE2	RN1	JE2	RN1	JE2
A-S30	> 1024	> 1024	> 75	> 75	< 0.1	< 0.1	< 1	< 1
A-T30	128	256	10	20	1	0.5	> 8	> 4
A-D30	64	128	5	10	> 16	> 8	> 16	> 8
G-S30	> 1024	> 1024	> 75	> 75	< 0.1	< 0.1	< 1	< 1
G-T30	128	128	10	10	0.3	0.3	4	4
G-D30	64	64	5	5	16	16	5	5

[a] MIC is the minimum inhibitory concentration at which no visible bacteria growth can be observed.

[b] Selectivity: lowest value between HC_{10} and c_H (hemocompatibility concentration) divided by the MIC of the bacterial strains concerned.

[c] Therapeutic index (TI) was calculated as the HaCaT IC_{50} of the SAMP to the MIC of the bacteria species.

3.5. Interactions of the guanidinium polymers with bacterial membrane

The variation in the MIC values between G-S30, G-T30 and G-D30 could either be explained by a difference in binding or ability to disrupt bacterial membrane. In order to determine if the binding efficiency between bacteria and guanidinium copolymers was influenced by monomer distribution, the Bodipy-functionalized guanidinium polymers were utilized. In mass concentration, the MIC of the fluorescent polymers were double that of their unlabelled counterparts (256 and 128 μg.mL^{-1} for G-T30^{Bodipy} and G-D30^{Bodipy}, respectively) as shown in Table SI-9. Although the MIC values of the fluorescent polymers (in molar concentration) against both RN1 and JE2 were slightly higher to that of the unlabelled polymers, the polymers maintained a significant antimicrobial activity after incorporation of BodipyAM, in turn validating the observations of the experiment (Table SI-9). The MRSA strain JE2 was incubated at 37 °C with each polymer at a concentration of 128 μg.mL^{-1} for 15, 30 and 120 minutes (Figure 4). For the 30 and 120 minute time points, propidium iodide (PI), which stains bacteria possessing a compromised membrane, was added 15 minutes prior to the end of the experiments. As there was no staining with PI for the 15 minute time point, in order to demonstrate that the bacterial binding of guanidinium polymers is independent of the presence of PI, Figure 4A displays only the brightfield (BF) and green channel (including a merge of the two). Microscopy revealed that G-D30^{Bodipy} clearly attached to bacteria within 15 minutes of incubation as illustrated in Figure 4A. According to the BF image, the bacteria appeared to be compromised in the presence of G-D30^{Bodipy}, as the shape of the majority of the bacterial population is poorly defined. In contrast, G-S30^{Bodipy} and G-T30^{Bodipy} did

not appear to bind bacteria as effectively within this timeframe, evidenced by the absence of noticeable fluorescence in the green channel. Additionally, the shape of the bacteria remained intact, indicating that the polymers did not compromise bacterial membrane.

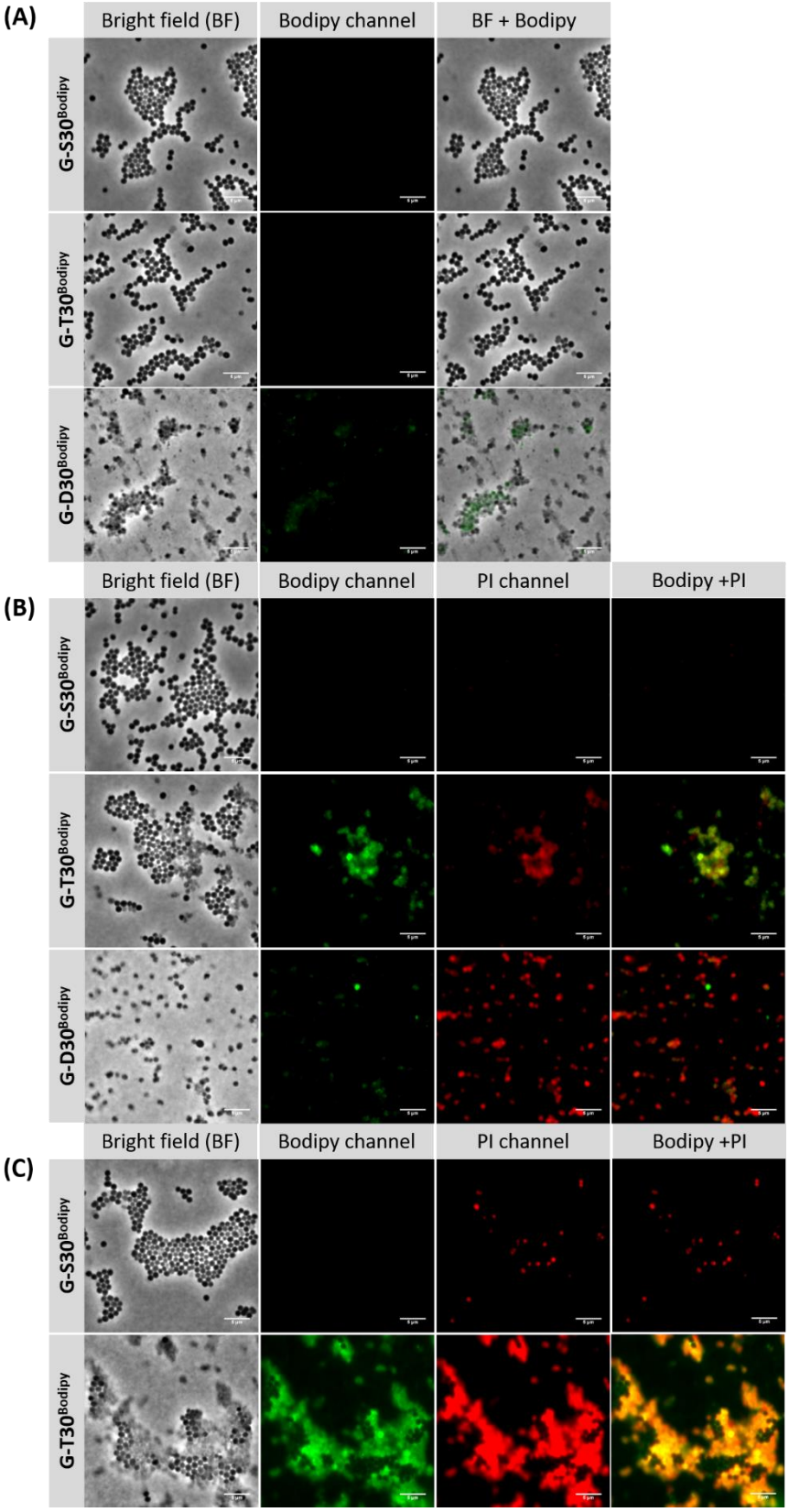

Figure 4. Bacterial membrane interactions of SAMPs. Binding assay with JE2 of the guanidinium SAMPs after 15 minutes without PI (A) Binding assay with JE2 after 30 minutes in presence of PI (B) Binding assay with JE2 after 2 hours in presence of PI, no image was presented for G-D30 after 2 hours no bacteria were left under these conditions (C). The scale bar represents 5 µm.

For the 30 minute time-point, Figure 4B displays images from the BF, Bodipy, PI channels and a merge of the Bodipy and PI channels. Following 30 minutes of incubation, both G-T30^{Bodipy} and G-D30^{Bodipy} bound to bacteria. Although the fluorescence intensity appeared to be greater following incubation with G-T30^{Bodipy} than G-D30^{Bodipy} for this time point, the BF images reveal that the number of bacteria was significantly lower following treatment with G-D30^{Bodipy}. Furthermore, after 30 minutes in presence of G-D30^{Bodipy}, most of the visible bacteria possess polymer bound to their surface and a compromised membrane, as can be seen with the overlay image of the Bodipy and PI channels, and are unhealthy, as indicated by their shape (BF). These pores would allow the polymers to diffuse out of the cell, which could explain a reduction in fluorescence intensity. Interestingly, bacteria interacting with G-T30^{Bodipy} were also exclusively the ones stained by PI. These results are in contradiction to a study from Tew *et al.*, which investigated the effect of guanidinium-functional polyoxanorbornene on the membrane integrity of *S. aureus* using PI.[42] Although the polymer showed a bactericidal effect against *S. aureus*, none of the bacteria were stained with PI after 30 minutes, indicating that bacterial membrane was not compromised. Comparable observations were reported by Good and co-workers after treatment of *E.coli* with PHMB. No permeability of bacterial membrane was observed in presence of PHMB after 60 minutes at 37 °C, when using SYTOX® Green as a membrane integrity probe, despite the potency of the polymer against *E. coli*. Following this experiment, it was suggested that complexation of PHMB with bacterial DNA was responsible for the antimicrobial character of the polymer, which could also be the mechanism of action of guanidinium-functional polyoxanorbornene.[67] The disruption of membrane integrity associated with G-T30^{Bodipy} and G-D30^{Bodipy} could be due to the action of the isopropyl groups of the NIPAM units - the polyoxanorbornene and PHMB did not bear any pendant alkyl chains, hence could likely cross bacterial membrane without compromising it.[42] In the present case, both pore formation and bacterial DNA binding could be occurring and collectively contributing towards bacterial death.

Following incubation with G-D30^{Bodipy} for 2 hours, no bacteria were observed, most probably because they were killed and subsequently removed during the washing step. In the presence of G-T30^{Bodipy} more bacteria were stained after 2 hours of incubation, compared to 30 minutes (Figure 4C). Again, co-localisation between G-T30^{Bodipy} and PI reinforces the previous observation that membrane disruption is a consequence of polymer binding. The BF image confirms the loss in membrane integrity for the majority of bacteria following 2 hours of incubation with G-T30^{Bodipy}. Although no bacteria were stained by G-S30^{Bodipy}, even after 2 hours, a few of them were stained with PI. A negative control

experiment with PBS and PI was performed and no membrane disruption was found (Figure SI-16). Therefore, in the case of G-S30^{Bodipy}, the statistical copolymer would have interacted with JE2 over the course of 2 hours, hence inducing membrane disruption, but to a limited extent.

In summary, G-D30^{Bodipy} underwent stronger interactions with the bacteria compared to G-T30^{Bodipy} (within 15 to 30 minutes, respectively), whilst G-S30^{Bodipy} only had limited interactions with JE2 even after 2 hours (Figure 4C). This trend correlates with the MIC values, as the tested concentration (128 μg.mL^{-1}) corresponds to the MIC of G-D30^{Bodipy} and half that of G-T30^{Bodipy} (G-S30^{Bodipy} was not active up to 1000 μg.mL^{-1}).

3.6. Synthesis and properties of guanidinium homopolymers

The difference in the MIC values of the guanidinium polymers could be explained by the fact that a minimum length of the cationic block is required for the polymer to interact with bacterial membrane. To test this hypothesis, guanidinium homopolymers of DP 15 and 30, which corresponds to the DP of the cationic block of G-T30 and G-D30, respectively, were synthesized. Similarly to the NIPAM copolymers, polyGEAM$_{15}$ and polyGEAM$_{30}$ were obtained by RAFT polymerization of diBocGEAM followed by hydrolysis to remove the Boc protecting groups (Tables SI-10 and SI-11, Figures SI-17, SI-18 and SI-19).

The antimicrobial activity of the homopolymers was tested against RN1 and JE2 (Figure 5A, Table SI-12). In the case of the homopolymers, the MIC of polyGEAM$_{15}$ and polyGEAM$_{30}$ were similar, meaning that the DP did not seem to affect the antimicrobial activity, and a cationic block of DP 15 was sufficient to allow interactions with bacterial membrane. However, as G-T30 did not bind as efficiently to bacteria as G-D30 (Figure 4), it is plausible that the polyNIPAM block sterically hinders the interaction of the polyGEAM block with bacterial membrane in the tetrablock structure.

The effect of the isopropyl moieties on the antimicrobial activity of the copolymers was evaluated by comparing the potency of the copolymers with the cationic homopolymers of similar polyGEAM length. If the hydrophobic chains are considered as “non-active” towards bacteria, the standard MIC values should be corrected to account for the content of charged “active” moieties of the respective polymers by multiplying the MIC expressed in molar concentration with the molar percentage of guanidinium functionalities in each polymer. According to Figure 5A, the re-evaluated MIC of G-T30 and G-D30 was less than half that of polyGEAM$_{15}$ and polyGEAM$_{30}$, respectively. This suggests that the polyNIPAM blocks participate in the antimicrobial activity of the polymers.

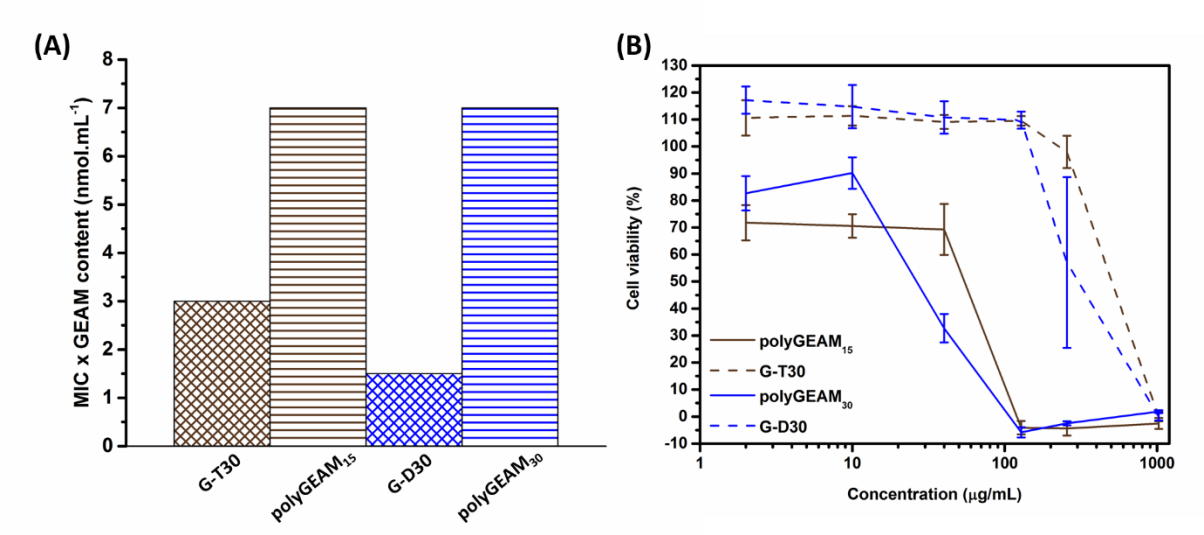

Figure 5. Antimicrobial activity and cytotoxicity of the guanidinium homopolymers. (A) Corrected MIC of polyGEAM and the guanidinium block copolymers against MRSA strain JE2 obtained by multiplying the MIC expressed in molar concentration with the molar percentage of guanidinium functionalities in each polymer. (B) Viability of HaCaT cells incubated for 24 hours in presence of guanidinium homopolymers and their associated copolymers using an XTT assay.

Additionally, the incorporation of NIPAM rendered the polymers less toxic *in vitro* towards mammalian cells as the cationic homopolymers were toxic at lower concentrations. Indeed, not only did they induce hemagglutination (from as low as 2 $\mu g.mL^{-1}$), but they were also hemolytic (Figure SI-20 and Table SI-13). To further investigate the toxicity against mammalian cells, HaCaT cells have been utilized and the IC_{50} was as low as 30 and 60 $\mu g.mL^{-1}$ for $polyGEAM_{30}$ and $polyGEAM_{15}$, respectively (Figure 5B).

3.7. Effect of segmentation on cell uptake of guanidinium copolymers

The potency of the SAMPs on intracellular bacteria strongly depends on their ability to enter mammalian cells. The uptake of the guanidinium-rich polymers by keratinocytes was studied to elucidate the effect of monomer distribution on their internalisation. For this assay, HaCaT cells were incubated with the fluorescent polymers at 128 $\mu g.mL^{-1}$ for 2 and 16 hours at 37 °C, and the levels of uptake were quantified for each compound (Figure 6, Table SI-14). Similar cellular fluorescence was observed with G-S30, G-T30 and G-D30 for both 2 and 16 hours. For this system, segmentation does not seem to have a significant impact on the internalisation in HaCaT cells. In a previous work using guanidinium polymers, we found a decrease in cell uptake with an increase in segmentation of functionalities (from statistical to tetrablock to diblock).[32] This discrepancy could be explained by the hydrophobicity of the co-monomer as the prior study used *N,N'*-dimethylacrylamide (DMA) and hydroxyethylacrylamide (HEA) copolymers. Indeed, there is strong evidence the hydrophobicity of cationic polymers influences the cell uptake mechanism.[70]

The uptake of the guanidinium polymers was further investigated by incubating the cells at 4 °C for 2 hours. At this temperature, not only would the internalisation *via* endocytosis be prevented, but the overall hydrophilicity of the SAMPs would decrease as the LCST of polyNIPAM is around 37 °C.[53] The internalisation of all three polymers was drastically reduced at 4 °C by over 70 % compared to that at 37 °C, indicating that the guanidinium polymers were taken up *via* both membrane permeation and endocytosis within HaCaT cells.[32] Although a decrease in internalisation was also observed with the DMA and HEA copolymers, the difference in cellular uptake at 37 and 4 °C was not as substantial, suggesting that a decrease in hydrophobicity of poly(GEAM-*co*-NIPAM) would also partly explain the reduction in cellular uptake at 4 °C. Moreover, the levels of uptake at 4 °C were comparable for G-S30, G-T30 and G-D30. As a result, all three SAMPs would be present in both endosomes and the cytosol, as demonstrated with the DMA and HEA copolymers using confocal microscopy.[32] Nonetheless, the guanidinium containing polymers are very likely to escape from endosomes due to their highly charged nature, as established with arginine-rich peptides, hence interact with bacteria present in the cytosol.[71-72]

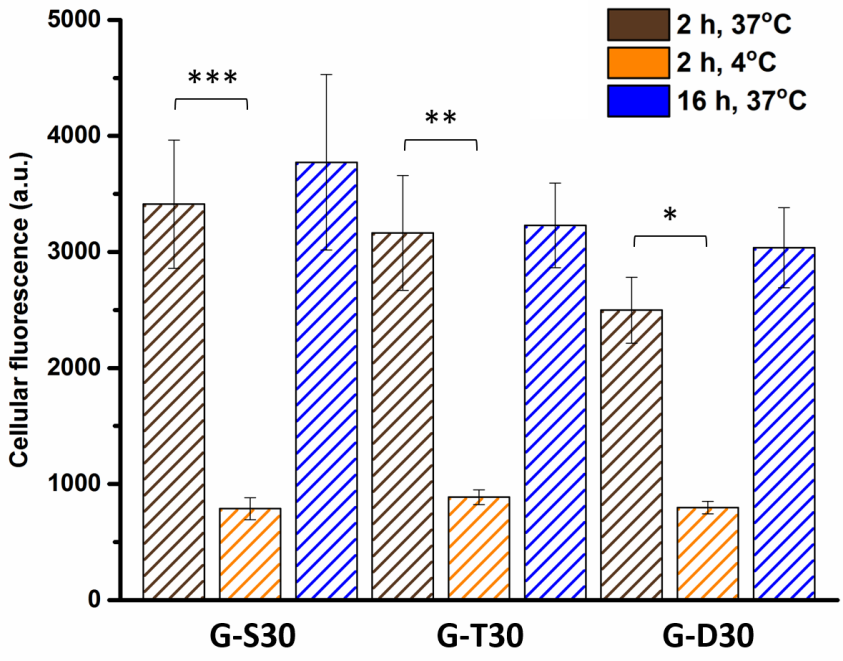

Figure 6. Comparison of cell uptake of guanidinium polymers with architecture. Cellular fluorescence measured for HaCaT cells in presence of 128 µg.mL^{-1} of fluorescent guanidinium polymers for the indicated time and temperature. *: $p \leq 0.05$; **: $p \leq 0.01$; ***: $p \leq 0.001$.

3.8. Effect of segmentation on potency against intracellular bacteria

Since the antimicrobial effect of the guanidinium polymers was studied in addition to their internalisation into mammalian cells, their activity against intracellular bacteria was then explored. In order to do so, HaCaT cells were infected with RN1 or JE2 for 2 hours and were then treated with a mixture of gentamicin and lysostaphin to kill extracellular bacteria as described in the literature.[73] Finally, the cells were incubated with the guanidinium compounds at a non-cytotoxic concentration of 128 $\mu g.mL^{-1}$ for 2 hours. Lysostaphin was used as a negative control as this enzyme is known to be ineffective against intracellular bacteria while killing any extracellular bacteria, which can be released by infected cells.[3] At the end of the polymer treatment, the cells were lysed, diluted, and plated to obtain bacterial counts (Figure 7).

Similar levels of intracellular MSSA RN1 were recovered with G-S30 and G-T30 compared to lysostaphin, meaning that the polymers would have inhibited the proliferation of extracellular bacteria released during the treatment. This would help containing the infection to an extent but would not be sufficient to treat infections. Interestingly, G-D30 was the most active for intracellular RN1, reducing the number of bacteria by two-fold compared to lysostaphin (Figure 7A). Similarly, G-D30 was active against intracellular JE2 with only half of the intracellular bacteria surviving compared to the lysostaphin, G-S30 and G-T30 treatments (Figure 7B). Although all three compounds were shown to be taken up in keratinocytes at similar levels (Figure 6), G-D30 exhibited the highest antimicrobial activity towards both RN1 and JE2 (Figure 3A and B), hence a corresponding increased intracellular killing efficiency compared to its statistical and tetrablock counterparts.

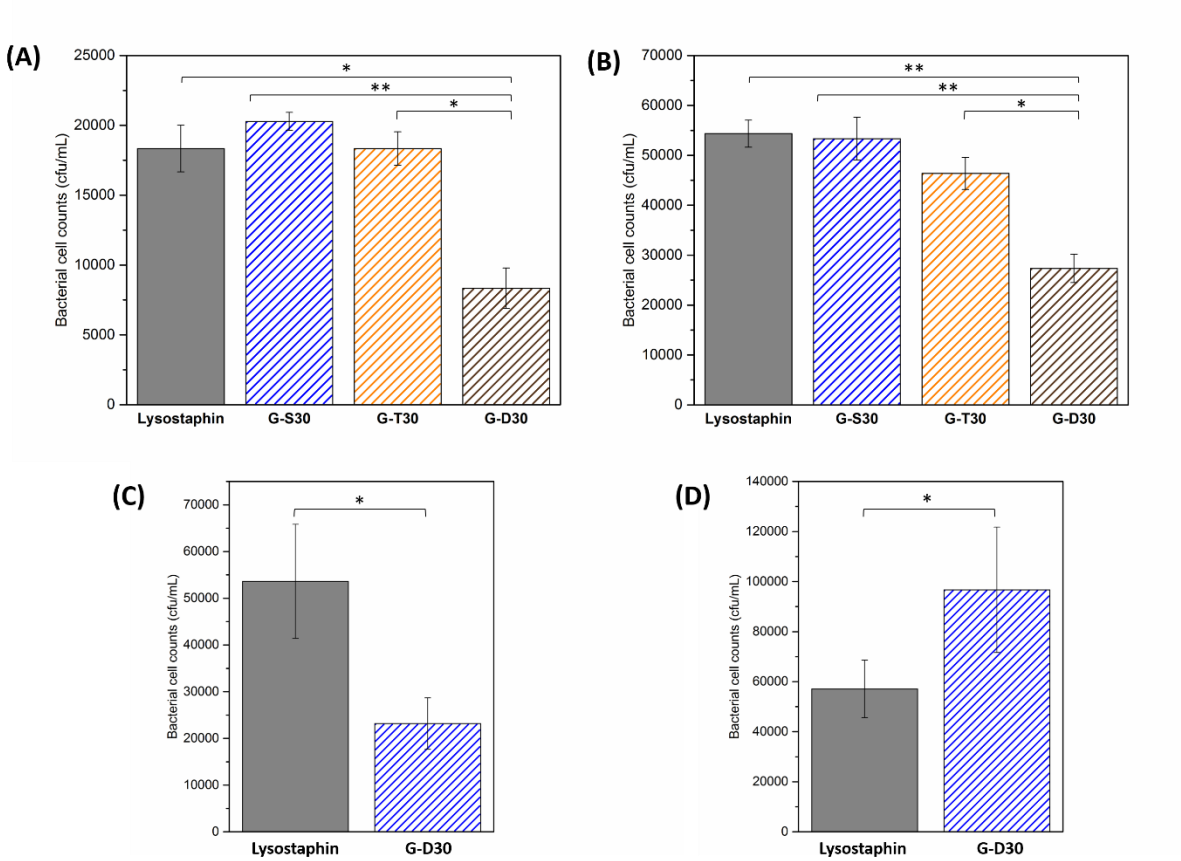

Figure 7. Intracellular activity of guanidinium polymers in HaCaT cells. Bacterial colony counts of intracellular bacteria after a polymer treatment at 128 µg.mL^{-1} for 2 hours against RN1 (A) and JE2 (B). Treatment with G-D30 at 40 µg.mL^{-1} for 2 hours against RN1 (C) and JE2 (D). *: $p \leq 0.05$; **: $p \leq 0.01$; ***: $p \leq 0.001$.

Since G-D30 was active against intracellular bacteria at 128 µg.mL^{-1}, it was also tested at 40 µg.mL^{-1} for 2 hours. G-D30 induced a similar inhibition level of 50 % against RN1 at the lower concentration (Figure 7C). However, the guanidinium diblock was not effective against intracellular JE2 at 40 µg.mL^{-1} (Figure 7D). A possible explanation could be that, as previously discussed, JE2 is less susceptible to SAMPs compared to RN1 due to its resistance to methicillin. As G-D30 did not exhibit any toxicity at 128 µg.mL^{-1} against the various types of human cells tested, it may be a promising therapeutic candidate for extracellular and intracellular killing of MRSA and MSSA.

4. Conclusion

Ammonium and guanidinium copolymers containing NIPAM as co-monomer were successfully synthesized *via* RAFT polymerization. By varying both the nature of the cationic functionality and the monomer distribution (statistical, tetrablock and diblock copolymers), the effect of charge and

segregation of functionalities on the biological properties of SAMPs was elucidated with both sets of polymers. Although the diblock copolymers exhibited a slightly higher toxicity towards epithelial cells than their statistical and tetrablock counterparts, they were associated with an improved hemocompatibility by a reduced hemagglutination activity. More importantly, segregation of the cationic and hydrophobic functionalities drastically improved the potency against *S. aureus*.

The diblock guanidinium polymer G-D30 particularly attracted our interest as it inhibited the growth of both intracellular MSSA and MRSA by 50 % over 2 hours. Its statistical and tetrablock analogues did not show any activity towards intracellular *S. aureus* although they were shown to be internalized at similar level as G-D30 *via* both active and passive mechanisms. Indeed, G-D30 was demonstrated to be the most efficient at attaching to bacterial membrane, followed by G-T30, whilst no binding was observed with G-S30. This reduced interaction could be attributed to the isopropyl functionalities hindering the guanidinium moieties from interacting with the negatively charged phospholipids present on bacterial membranes. Nonetheless, there is strong evidence that these hydrophobic functionalities are key for both the antimicrobial activity and the internalisation into mammalian cells. The isopropyl functionalities from the polyNIPAM block of G-D30 and G-T30 were probably responsible for permeabilising bacterial membrane as previous work with guanidinium containing homopolymers did not demonstrate this property. Therefore, the optimized sequence for the killing of intracellular and extracellular MRSA appears to be the guanidinium diblock copolymer structure, which could find applications in the treatment of infections, whilst limiting antibiotic induced-bacterial resistance.[2] In order to further reduce the amount of intracellular bacteria, variation in the hydrophobic functionality or overall charge content could be investigated.

Acknowledgements

The CSIRO PhD scholarship scheme (AK), the CSIRO Julius Career Award (KL) and the German Research Foundation (DFG, GZ: HA 7725/1-1) (MH) as well as the Royal Society Wolfson Merit Award (WM130055; SP), and the Monash-Warwick Alliance (SP), are acknowledged for funding.

Competing interests

The authors declare no competing financial interests.

References

1. Köck, R.; Becker, K.; Cookson, B.; van Gemert-Pijnen, J. E.; Harbarth, S.; Kluytmans, J., et al., Systematic literature analysis and review of targeted preventive measures to limit healthcare-associated infections by meticillin-resistant Staphylococcus aureus. Euro Surveillance 2014; 19:20860.
2. Annual epidemiological report : Antimicrobial resistance and health care-associated infections In European Centre For Disease Prevention And Control, 2014.
3. Garzoni, C.; Kelley, W. L., *Staphylococcus aureus*: new evidence for intracellular persistence. Trends in Microbiology 2009; 17:59-65.

4. Singer, A. J.; Talan, D. A., Management of Skin Abscesses in the Era of Methicillin-Resistant Staphylococcus aureus. 2014; 370:1039-1047.
5. Lubritz, G.; Peters, G.; Becker, K.; von Eiff, C.; Metze, D.; Hockmann, J., et al., Intracellular Persistence of Staphylococcus aureus Small-Colony Variants within Keratinocytes: A Cause for Antibiotic Treatment Failure in a Patient with Darier's Disease. Clinical Infectious Diseases 2001; 32:1643-1647.
6. Soong, G.; Paulino, F.; Wachtel, S.; Parker, D.; Wickersham, M.; Zhang, D., et al., Methicillin-resistant Staphylococcus aureus adaptation to human keratinocytes. mBio 2015; 6:e00289-15.
7. Zautner, A. E.; Krause, M.; Stropahl, G.; Holtfreter, S.; Frickmann, H.; Maletzki, C., et al., Intracellular Persisting Staphylococcus aureus Is the Major Pathogen in Recurrent Tonsillitis. PLOS ONE 2010; 5:e9452.
8. Chaponnier, C.; Kampf, S.; Clement, S.; Lew, D.; Huggler, E.; Schrenzel, J., et al., Evidence of an Intracellular Reservoir in the Nasal Mucosa of Patients with Recurrent Staphylococcus aureus Rhinosinusitis. The Journal of Infectious Diseases 2005; 192:1023-1028.
9. Krut, O.; Sommer, H.; Krönke, M., Antibiotic-induced persistence of cytotoxic Staphylococcus aureus in non-phagocytic cells. Journal of Antimicrobial Chemotherapy 2004; 53:167-173.
10. Bastos, M. d. C. d. F.; Coutinho, B. G.; Coelho, M. L. V., Lysostaphin: A Staphylococcal Bacteriolysin with Potential Clinical Applications. Pharmaceuticals 2010; 3:1139.
11. Pinto-Alphandary, H.; Andremont, A.; Couvreur, P., Targeted delivery of antibiotics using liposomes and nanoparticles: research and applications. International Journal of Antimicrobial Agents 2000; 13:155-168.
12. Sémiramoth, N.; Meo, C. D.; Zouhiri, F.; Saïd-Hassane, F.; Valetti, S.; Gorges, R., et al., Self-Assembled Squalenoylated Penicillin Bioconjugates: An Original Approach for the Treatment of Intracellular Infections. ACS Nano 2012; 6:3820-3831.
13. Lutwyche, P.; Cordeiro, C.; Wiseman, D. J.; St-Louis, M.; Uh, M.; Hope, M. J., et al., Intracellular delivery and antibacterial activity of gentamicin encapsulated in pH-sensitive liposomes. Antimicrobial agents and chemotherapy 1998; 42:2511-2520.
14. Boonyarattanakalin, S.; Hu, J.; Dykstra-Rummel, S. A.; August, A.; Peterson, B. R., Endocytic Delivery of Vancomycin Mediated by a Synthetic Cell Surface Receptor: Rescue of Bacterially Infected Mammalian Cells and Tissue Targeting In Vivo. J. Am. Chem. Soc. 2007; 129:268-269.
15. Nepal, M.; Mohamed, M. F.; Blade, R.; Eldesouky, H. E.; N. Anderson, T.; Seleem, M. N., et al., A Library Approach to Cationic Amphiphilic Polyproline Helices that Target Intracellular Pathogenic Bacteria. ACS Infectious Diseases 2018; 4:1300-1305.
16. Lei, E. K.; Pereira, M. P.; Kelley, S. O., Tuning the Intracellular Bacterial Targeting of Peptidic Vectors. Angew. Chem. Int. Ed. 2013; 52:9660-9663.
17. Yang, S.; Han, X.; Yang, Y.; Qiao, H.; Yu, Z.; Liu, Y., et al., Bacteria-Targeting Nanoparticles with Microenvironment-Responsive Antibiotic Release To Eliminate Intracellular Staphylococcus aureus and Associated Infection. ACS Appl. Mater. Interfaces 2018; 10:14299-14311.
18. Laxminarayan, R.; Duse, A.; Wattal, C.; Zaidi, A. K. M.; Wertheim, H. F. L.; Sumpradit, N., et al., Antibiotic resistance—the need for global solutions. The Lancet Infectious Diseases 2013; 13:1057-1098.
19. Ellington, J. K.; Harris, M.; Hudson, M. C.; Vishin, S.; Webb, L. X.; Sherertz, R., Intracellular Staphylococcus aureus and antibiotic resistance: Implications for treatment of staphylococcal osteomyelitis. Journal of Orthopaedic Research 2006; 24:87-93.
20. Zasloff, M., Antimicrobial peptides of multicellular organisms. Nature 2002; 415:389-395.
21. Ganewatta, M. S.; Tang, C., Controlling macromolecular structures towards effective antimicrobial polymers. Polymer 2015; 63:A1-A29.
22. Cao, B.; Xiao, F.; Xing, D.; Hu, X., Polyprodrug Antimicrobials: Remarkable Membrane Damage and Concurrent Drug Release to Combat Antibiotic Resistance of Methicillin-Resistant Staphylococcus aureus. Small 2018; 14:1802008.
23. Li, Y.; Yu, H.; Qian, Y.; Hu, J.; Liu, S., Amphiphilic Star Copolymer-Based Bimodal Fluorogenic/Magnetic Resonance Probes for Concomitant Bacteria Detection and Inhibition. Adv. Mater. 2014; 26:6734-6741.
24. Li, Y.; Liu, G.; Wang, X.; Hu, J.; Liu, S., Enzyme-Responsive Polymeric Vesicles for Bacterial-Strain-Selective Delivery of Antimicrobial Agents. Angew. Chem. Int. Ed. 2016; 55:1760-1764.
25. Huang, K.-S.; Yang, C.-H.; Huang, S.-L.; Chen, C.-Y.; Lu, Y.-Y.; Lin, Y.-S., Recent Advances in Antimicrobial Polymers: A Mini-Review. International journal of molecular sciences 2016; 17:1578.
26. Van Bambeke, F.; Mingeot-Leclercq, M.-P.; Struelens, M. J.; Tulkens, P. M., The bacterial envelope as a target for novel anti-MRSA antibiotics. Trends in Pharmacological Sciences 2008; 29:124-134.
27. Hartlieb, M.; Williams, E. G. L.; Kuroki, A.; Perrier, S.; Locock, K. E. S., Antimicrobial Polymers: Mimicking Amino Acid Functionali ty, Sequence Control and Three-dimensional Structure of Host-defen se Peptides. Current Medicinal Chemistry 2017; 24:2115-2140.

28. Treat, N. J.; Smith, D.; Teng, C.; Flores, J. D.; Abel, B. A.; York, A. W., et al., Guanidine-Containing Methacrylamide (Co)polymers via aRAFT: Toward a Cell Penetrating Peptide Mimic. ACS macro letters 2012; 1:100-104.
29. Wender, P. A.; Mitchell, D. J.; Pattabiraman, K.; Pelkey, E. T.; Steinman, L.; Rothbard, J. B., The design, synthesis, and evaluation of molecules that enable or enhance cellular uptake: peptoid molecular transporters. Proceedings of the National Academy of Sciences of the United States of America 2000; 97:13003-13008.
30. Cooley, C. B.; Trantow, B. M.; Nederberg, F.; Kiesewetter, M. K.; Hedrick, J. L.; Waymouth, R. M., et al., Oligocarbonate Molecular Transporters: Oligomerization-Based Syntheses and Cell-Penetrating Studies. J. Am. Chem. Soc. 2009; 131:16401-16403.
31. Wender, P. A.; Galliher, W. C.; Goun, E. A.; Jones, L. R.; Pillow, T. H., The design of guanidinium-rich transporters and their internalization mechanisms. Advanced Drug Delivery Reviews 2008; 60:452-472.
32. Martin, L.; Peltier, R.; Kuroki, A.; Town, J. S.; Perrier, S., Investigating Cell Uptake of Guanidinium-Rich RAFT Polymers: Impact of Comonomer and Monomer Distribution. Biomacromolecules 2018; 19:3190-3200.
33. Herce, H. D.; Garcia, A. E.; Cardoso, M. C., Fundamental Molecular Mechanism for the Cellular Uptake of Guanidinium-Rich Molecules. J. Am. Chem. Soc. 2014; 136:17459-17467.
34. Locock, K. E. S.; Michl, T. D.; Valentin, J. D. P.; Vasilev, K.; Hayball, J. D.; Qu, Y., et al., Guanylated Polymethacrylates: A Class of Potent Antimicrobial Polymers with Low Hemolytic Activity. Biomacromolecules 2013; 14:4021-4031.
35. Kamaruzzaman, N. F.; Firdessa, R.; Good, L., Bactericidal effects of polyhexamethylene biguanide against intracellular Staphylococcus aureus EMRSA-15 and USA 300. Journal of Antimicrobial Chemotherapy 2016; 71:1252-1259.
36. Ansorg, R.; Rath, P.-M.; Fabry, W., Inhibition of the Anti-staphylococcal Activity of the Antiseptic Polihexanide by Mucin. Arzneimittelforschung 2003; 53:368-371.
37. Opinion on Polyaminopropyl Biguanide (PHMB). Submission III ed.; European Commission, 2017.
38. Judzewitsch, P. R.; Nguyen, T.-K.; Shanmugam, S.; Wong, E. H. H.; Boyer, C., Towards Sequence-Controlled Antimicrobial Polymers: Effect of Polymer Block Order on Antimicrobial Activity. Angew. Chem. Int. Ed. 2018; 57:4559-4564.
39. Kuroki, A.; Sangwan, P.; Qu, Y.; Peltier, R.; Sanchez-Cano, C.; Moat, J., et al., Sequence Control as a Powerful Tool for Improving the Selectivity of Antimicrobial Polymers. ACS Appl. Mater. Interfaces 2017; 9:40117-40126.
40. Budhathoki-Uprety, J.; Peng, L.; Melander, C.; Novak, B. M., Synthesis of Guanidinium Functionalized Polycarbodiimides and Their Antibacterial Activities. ACS Macro Letters 2012; 1:370-374.
41. Sarapas, J. M.; Backlund, C. M.; deRonde, B. M.; Minter, L. M.; Tew, G. N., ROMP- and RAFT-Based Guanidinium-Containing Polymers as Scaffolds for Protein Mimic Synthesis. Chemistry (Weinheim an der Bergstrasse, Germany) 2017; 23:6858-6863.
42. Gabriel, G. J.; Madkour, A. E.; Dabkowski, J. M.; Nelson, C. F.; Nüsslein, K.; Tew, G. N., Synthetic Mimic of Antimicrobial Peptide with Nonmembrane-Disrupting Antibacterial Properties. Biomacromolecules 2008; 9:2980-2983.
43. Perrier, S., 50th Anniversary Perspective: RAFT Polymerization—A User Guide. Macromolecules 2017; 50:7433-7447.
44. Moad, G.; Rizzardo, E.; Thang, S. H., Living Radical Polymerization by the RAFT Process – A Third Update. Australian Journal of Chemistry 2012; 65:985-1076.
45. Kuroki, A.; Martinez-Botella, I.; Hornung, C. H.; Martin, L.; Williams, E. G. L.; Locock, K. E. S., et al., Looped flow RAFT polymerization for multiblock copolymer synthesis. Polym. Chem. 2017; 8:3249-3254.
46. Gody, G.; Maschmeyer, T.; Zetterlund, P. B.; Perrier, S., Exploitation of the Degenerative Transfer Mechanism in RAFT Polymerization for Synthesis of Polymer of High Livingness at Full Monomer Conversion. Macromolecules 2014; 47:639-649.
47. Gody, G.; Zetterlund, P. B.; Perrier, S.; Harrisson, S., The limits of precision monomer placement in chain growth polymerization. Nature Communications 2016; 7:10514.
48. Gody, G.; Maschmeyer, T.; Zetterlund, P. B.; Perrier, S., Pushing the Limit of the RAFT Process: Multiblock Copolymers by One-Pot Rapid Multiple Chain Extensions at Full Monomer Conversion. Macromolecules 2014; 47:3451-3460.
49. Martin, L.; Gody, G.; Perrier, S., Preparation of complex multiblock copolymers via aqueous RAFT polymerization at room temperature. Polym. Chem. 2015; 6:4875-4886.
50. Smets, G.; Hesbain, A. M., Hydrolysis of polyacrylamide and acrylic acid–acrylamide copolymers. Journal of Polymer Science 1959; 40:217-226.

51. Peltier, R.; Bialek, A.; Kuroki, A.; Bray, C.; Martin, L.; Perrier, S., Reverse-phase high performance liquid chromatography (RP-HPLC) as a powerful tool to characterise complex water-soluble copolymer architectures. Polym. Chem. 2018; 9:5511-5520.
52. Hou, L.; Wu, P., Comparison of LCST-transitions of homopolymer mixture, diblock and statistical copolymers of NIPAM and VCL in water. Soft Matter 2015; 11:2771-2781.
53. Wei, H.; Cheng, S.-X.; Zhang, X.-Z.; Zhuo, R.-X., Thermo-sensitive polymeric micelles based on poly(N-isopropylacrylamide) as drug carriers. Progress in Polymer Science 2009; 34:893-910.
54. Feil, H.; Bae, Y. H.; Feijen, J.; Kim, S. W., Effect of comonomer hydrophilicity and ionization on the lower critical solution temperature of N-isopropylacrylamide copolymers. Macromolecules 1993; 26:2496-2500.
55. Squeo, B. M.; Gregoriou, V. G.; Avgeropoulos, A.; Baysec, S.; Allard, S.; Scherf, U., et al., BODIPY-based polymeric dyes as emerging horizon materials for biological sensing and organic electronic applications. Progress in Polymer Science 2017; 71:26-52.
56. Summers, G. H.; Lefebvre, J.-F.; Black, F. A.; Stephen Davies, E.; Gibson, E. A.; Pullerits, T., et al., Design and characterisation of bodipy sensitizers for dye-sensitized NiO solar cells. Physical Chemistry Chemical Physics 2016; 18:1059-1070.
57. Fischer, D.; Li, Y.; Ahlemeyer, B.; Krieglstein, J.; Kissel, T., In vitro cytotoxicity testing of polycations: influence of polymer structure on cell viability and hemolysis. Biomaterials 2003; 24:1121-1131.
58. Locock, K. E. S.; Michl, T. D.; Stevens, N.; Hayball, J. D.; Vasilev, K.; Postma, A., et al., Antimicrobial Polymethacrylates Synthesized as Mimics of Tryptophan-Rich Cationic Peptides. ACS Macro Letters 2014; 3:319-323.
59. von Eiff, C.; Becker, K.; Metze, D.; Lubritz, G.; Hockmann, J.; Schwarz, T., et al., Intracellular Persistence of Staphylococcus aureus Small-Colony Variants within Keratinocytes: A Cause for Antibiotic Treatment Failure in a Patient with Darier's Disease. Clinical Infectious Diseases 2001; 32:1643-1647.
60. Exley, S. E.; Paslay, L. C.; Sahukhal, G. S.; Abel, B. A.; Brown, T. D.; McCormick, C. L., et al., Antimicrobial Peptide Mimicking Primary Amine and Guanidine Containing Methacrylamide Copolymers Prepared by Raft Polymerization. Biomacromolecules 2015; 16:3845-3852.
61. Bechara, C.; Sagan, S., Cell-penetrating peptides: 20 years later, where do we stand? FEBS Lett. 2013; 587:1693-1702.
62. Neamnark, A.; Suwantong, O.; K. C, R. B.; Hsu, C. Y. M.; Supaphol, P.; Uludağ, H., Aliphatic Lipid Substitution on 2 kDa Polyethylenimine Improves Plasmid Delivery and Transgene Expression. Molecular Pharmaceutics 2009; 6:1798-1815.
63. Rubinstein, E.; Kollef, M. H.; Nathwani, D., Pneumonia Caused by Methicillin-Resistant Staphylococcus aureus. Clinical Infectious Diseases 2008; 46:S378-S385.
64. Herbert, S.; Ziebandt, A.-K.; Ohlsen, K.; Schäfer, T.; Hecker, M.; Albrecht, D., et al., Repair of global regulators in Staphylococcus aureus 8325 and comparative analysis with other clinical isolates. Infection and immunity 2010; 78:2877-2889.
65. Bæk, K. T.; Gründling, A.; Mogensen, R. G.; Thøgersen, L.; Petersen, A.; Paulander, W., et al., β-Lactam resistance in methicillin-resistant Staphylococcus aureus USA300 is increased by inactivation of the ClpXP protease. Antimicrobial agents and chemotherapy 2014; 58:4593-4603.
66. Sakai, N.; Matile, S., Anion-Mediated Transfer of Polyarginine across Liquid and Bilayer Membranes. J. Am. Chem. Soc. 2003; 125:14348-14356.
67. Chindera, K.; Mahato, M.; Kumar Sharma, A.; Horsley, H.; Kloc-Muniak, K.; Kamaruzzaman, N. F., et al., The antimicrobial polymer PHMB enters cells and selectively condenses bacterial chromosomes. Scientific Reports 2016; 6:23121.
68. García, A. B.; Viñuela-Prieto, J. M.; López-González, L.; Candel, F. J., Correlation between resistance mechanisms in Staphylococcus aureus and cell wall and septum thickening. Infection and drug resistance 2017; 10:353-356.
69. Kawada-Matsuo, M.; Komatsuzawa, H., Factors affecting susceptibility of Staphylococcus aureus to antibacterial agents. Journal of Oral Biosciences 2012; 54:86-91.
70. Liu, Z.; Zhang, Z.; Zhou, C.; Jiao, Y., Hydrophobic modifications of cationic polymers for gene delivery. Progress in Polymer Science 2010; 35:1144-1162.
71. Varkouhi, A. K.; Scholte, M.; Storm, G.; Haisma, H. J., Endosomal escape pathways for delivery of biologicals. J. Control. Release 2011; 151:220-228.
72. Kamaruzzaman, N. F.; Chong, S. Q. Y.; Edmondson-Brown, K. M.; Ntow-Boahene, W.; Bardiau, M.; Good, L., Bactericidal and Anti-biofilm Effects of Polyhexamethylene Biguanide in Models of Intracellular and Biofilm of Staphylococcus aureus Isolated from Bovine Mastitis. Frontiers in microbiology 2017; 8:1518-1518.
73. Korea, C. G.; Balsamo, G.; Pezzicoli, A.; Merakou, C.; Tavarini, S.; Bagnoli, F., et al., Staphylococcal Esx proteins modulate apoptosis and release of intracellular Staphylococcus aureus during infection in epithelial cells. Infection and immunity 2014; 82:4144-4153.